

# ADSORPTION BEHAVIOR OF ANIONIC AND CATIONIC DYES ONTO SUGARCANE BAGASSE ACTIVATED CARBON

**Palanichamy Rajeshkanna <sup>a</sup>, Sankaran Meenakshi <sup>b\*</sup>, Natesan Nagarajan <sup>b\*</sup>**

*a Tamilnadu Newsprint and Papers Ltd, Kagithapuram, Karur- 639136, Tamilnadu, India.*

*b, \* Department of Chemistry, Gandhigram Rural Institute, Deemed to be University, Gandhigram -624302, Tamilnadu, India.*

**Abstract**—The present study deals with the feasibility of removal of an anionic dye acid orange (AO7) and a cationic dye Rhodamine B (RhB) from aqueous solutions using activated carbon derived from sugarcane bagasse. Batch adsorption studies were conducted to evaluate various experimental parameters such as contact time, initial concentration of the adsorbate, adsorbent dosage, pH and temperature for maximum sorption. Favorable adsorption of RhB occurs at around pH 4.0 and for AO7 maximum sorption was found to be at pH 2.0. The adsorption process is in conformity with Freundlich isotherm for both RhB and AO7. Different thermodynamic parameters such as Gibb's free energy, enthalpy and entropy of the on-going adsorption process have also been evaluated. The thermodynamic parameters of RhB adsorption indicated that the system was exothermic in nature and at the same time the adsorption process of AO7 was endothermic. Kinetic results suggest that the adsorption of RhB and AO7 onto Bagasse Activated Carbon (BAC) followed pseudo - second - order kinetic model.

**Keywords** — Adsorption, Isotherm, Sugarcane Bagasse, Rhodamine B, Acid Orange 7

## I. Introduction

Currently, textile industry produces a huge quantity of dyed wastewater. The color and the non-biodegradable nature of the spent dye baths constitute serious environmental problems [1]. Dyes and pigments represent one of the problematic groups; they are discharged into wastewaters from various industrial branches, mainly from the dye manufacturing, food coloring, cosmetic, paper, textile and carpet industries [2]. The complex aromatic structures of dyes make them more stable and more difficult to biodegrade [3].

The convectional biological treatment process is not very effective in treating a dyes wastewater, due to low biodegradation of dyes. It is usually treated by either physical or chemical Dye removal from aqueous solution using low cost adsorbent processes. However, these processes were very expensive and could not be effectively used to treat the wide range of dyes [4]. The removal of such colored agents from aqueous effluents is thus environmentally significant [5-10], and as certain industries like textile, pulp and paper produce bulk quantity of colored waste water, the production of an effective and cheap activated carbon from agricultural wastes is thus of economic and academic interest.

Adsorption technique is an important method in case of heterogeneous systems. To fully understand the processes, two basic ingredients are required, namely, equilibrium and kinetics. Recently, the growth of adsorption kinetics is of interest for many investigations [11-14].

The focus of the present study was to investigate the effect of the sorbent amount, contact time, dye concentration, and temperature on the adsorption of RhB and AO7 on BAC. Different isotherm models were used to derive the adsorption parameters for RhB and AO7 on BAC. The adsorption rate constants were obtained at different temperatures to estimate the thermodynamic parameters for the dye adsorption.

## II. MATERIALS AND METHODS

### II.1 Adsorbate and adsorbent

Sugarcane bagasse, as an adsorbent, was collected from local sugar mill, Karur. The collected material was thoroughly washed with distilled water and dried in oven at 105° C and then powdered by using pulveriser. Then the powder was modified as activated carbon and used for adsorption studies. Phosphoric acid (H<sub>3</sub>PO<sub>4</sub>) (Merck) 85% (wt) solution was used as the chemical activating agent. Rhodamine-B and Acid Orange 7 were procured from Merck with analytical grade. The chemical structures of the dyes were shown in **Fig 1**. All other chemicals were of analytical grade and obtained from Chemical Drug House (CDH) Ltd., India. The double distilled water (DD) was used to prepare all the aqueous solutions.

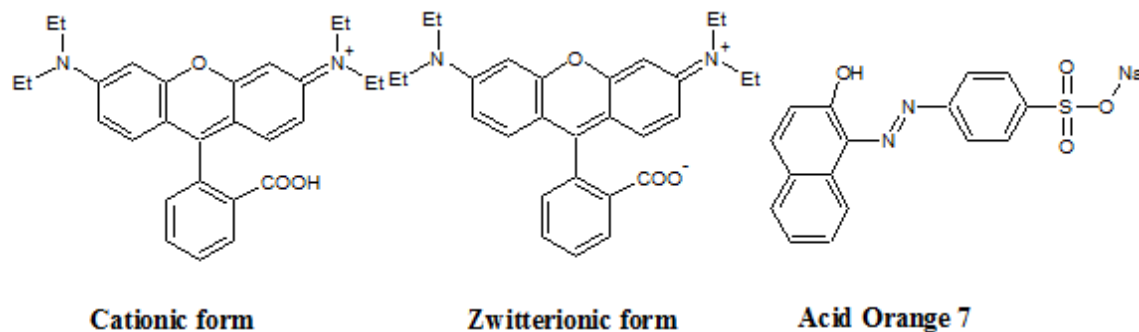


**Fig.1- Molecular forms of RhB (cationic and zwitterionic form) and AO7**

### II.2 Preparation of Activated carbon

Sugarcane bagasse was chosen as precursor for the production of activated carbon by one-step chemical activation. The crushed Sugarcane bagasse was soaked in a ratio of 1 :1.5 wt of bagasse /wt of H<sub>3</sub>PO<sub>4</sub> solution to cover it completely, slightly agitated to ensure penetration of the acid throughout, then the mixture was heated to 80°C for 1 h and left overnight at room temperature to help appropriate wetting and impregnation of the precursor. The impregnated mass was dried in an air oven at 80°C overnight, then, carbonized in a closed stainless steel reactor placed in a programmable muffle Furnace. The carbonization process was carried out at 500°C for 30 min in limited air. The product – (BAC) refers to H<sub>3</sub>PO<sub>4</sub> treatment – was thoroughly washed with warm distilled water (70°C) until pH of the solution came close to the initial pH of the rinsing water. Finally, the activated carbon was dried at 105°C for 24 h and sieved to different particle size by using ASTM mesh and accepted particle size of 40 μ was kept for use [15].

### II.3 Preparation of dye solutions

The stock solution of each dye was prepared by dissolving 1 g of analytical grade dyes in 1000 mL of distilled water and diluted to get desired concentration of the dyes. All experiments were carried out at room temperature (29±1°C) using a constant agitation speed of 100 rpm. The pH of each solution was adjusted to the required value with diluted or concentrated and Hydrochloric acid (HCl), sodium hydroxide (NaOH) solutions before contacting the adsorbent. Experimental solutions of the desired concentrations were prepared by successive dilutions. All the experiments were carried out in a batch system in order to evaluate the effects of different operational variables.

### II.4. Batch experiments

The batch experiments were performed in a 250 mL conical flask in which 0.1 g of the activated carbon was added to 50 mL of dye solutions. Then, the mixture was kept at room temperature (30°C) for the desired time under shaking at 300 rpm. After the desired time, the material was filtered through filter paper. The dyes concentrations were determined using absorbance values measured before and after the adsorption by UV-spectrophotometer (Pharo 300 Merck) at the wavelength corresponding to the maximum absorbance of 490 and 554 nm for AO7 and RhB, respectively. The maximum wavelength ( $\lambda_{\max}$ ) for both adsorbents was recorded by UV-vis

spectrophotometer. In all cases, a proper dilution was necessary to obtain a well measurable absorption. The pH of the solutions during the studies was determined by a pH meter.

To optimize the conditions for dye removal, and also to evaluate the adsorption capacity of BAC, the adsorption reactions were conducted at a wide pH range (pH 2–10), contact time (15–90 min), initial concentration (10–50 mg L<sup>-1</sup>), and adsorbent dose (0.020–0.140 g). The working solution pH was adjusted by adding 0.1M of HCl / NaOH. For isotherm studies, the experiments were carried out at three different temperatures with four different concentrations of dyes viz., 10, 20, 30 and 40 mg L<sup>-1</sup>. Thermodynamic parameters such as standard free energy change ( $\Delta G^0_{ads}$ ), standard enthalpy change ( $\Delta H^0_{ads}$ ) and standard entropy change ( $\Delta S^0_{ads}$ ) were determined using equilibrium data. Kinetic data were obtained by conducting experiments at 303K with three different concentrations of both the dyes. While doing the experiment, the samples were withdrawn at pre-determined time interval and analyzed for the dye concentration. The percent dye removal by BAC was computed using the following equation.

$$\text{Removal efficiency} = \frac{C_0 - C_e}{C_0} \times 100 \quad (1)$$

Where,  $C_0$  and  $C_e$  are the initial and final concentration of dye, respectively). The sorption capacity of the activated carbon was calculated according to the following mass balance Eq. (2):

$$\text{Sorption Capacity (SC)}, \quad q_t = \frac{(C_0 - C_e)}{M} \times V \quad (\text{mg/g}) \quad (2)$$

Where,  $q$  is the adsorption capacity of the composite (mg/g),  $V$  is the volume of the sample (mL),  $C_0$  is the initial concentration of dye solution (mg/L),  $C_e$  is the final concentration of dye solution (mg/L) and  $M$  is the mass (g) of the activated carbon.

### III. RESULTS AND DISCUSSION

#### III.1. Characterization of activated carbon

FTIR analyses on BAC before and after dye adsorption were conducted to further understand the adsorption chemistry. As shown in Fig. 2, for untreated BAC sample (2a), the intense band at around 3400- 3450 cm<sup>-1</sup> assigned to OH group stretching vibration and the absorption band at 2920 cm<sup>-1</sup> could be attributed to C-H aliphatic axial deformation in CH<sub>2</sub> and CH<sub>3</sub> groups from cellulose, lignin and hemicelluloses [11]. The band at 2852 cm<sup>-1</sup> is assignable C-H vibration of vibration of OCH<sub>3</sub> groups, which is commonly present in lignin. After dye adsorption, the band intensity at 3430 cm<sup>-1</sup> significantly reduced, probably indicating some interactions between OH groups in BAC and those of the dye functional groups. The small peaks located at (400 to 700) cm<sup>-1</sup> could be the C-H out-of-plane bending in benzene derivatives that is quite common for activated carbon. As can be seen in Fig. 2b, 2c the shift and sharp reduction (3397 and 3381 cm<sup>-1</sup>) suggests the major role of –OH group for RhB and AO7 adsorption onto BAC. [16]

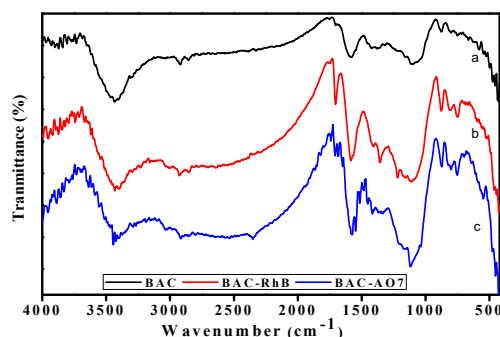


Fig.2- FTIR spectra of (a) BAC (b) RhB adsorbed BAC and (c) AO7 adsorbed BAC

The morphology of activated carbon was studied by SEM. Fig. 3 shows different views of activated carbon. Pores of different size and different shape could be observed in these figures.

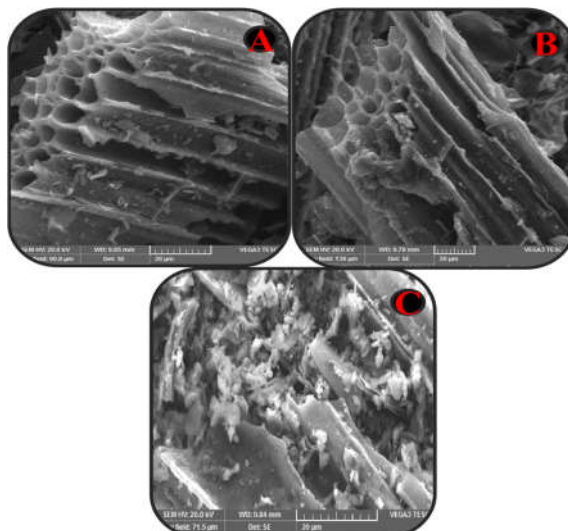


Fig.3- SEM micrographs of (a) BAC (b) RhB adsorbed BAC and (c) AO7 adsorbed BAC

### III.2. Effect of pH

The influence of solution pH on the removal of RhB and AO7 onto the BAC was studied and is illustrated in Fig. 4A. The pH measurements were carried out using the expandable ion analyzer EA 940 with pH electrode. The uptake of RhB at pH 10.0-12.0 was the minimum and a maximum uptake was obtained at pH 4.0. However, when the pH of the solution was increased (more than pH 4), the uptake of RhB was decreased. It appears that a change in pH of the solution results in the formation of different ionic species, and different carbon surface charge. At pH values lower than 4, the dye can enter into the pore structure. At a pH value higher than 4, the zwitterions form of RhB in water may increase the aggregation of RhB to form a bigger molecular form (dimmer) and become unable to enter into the pore structure of the carbon surface [17-19]. Due to the amphoteric character of a dye, its adsorption properties may be influenced by the pH value of the solution.

The experiments were carried out for AO7 also at different initial solution pH values varying from 2 to 10. The dye removal percentage of AO7 decreased significantly with an increase in the solution pH and the maximum adsorption level was determined at pH 2. It is well known that at lower pH, more protons will be available to protonate the adsorbent surface, thereby increasing the electrostatic attractions between negatively charged dye anions and positively charged adsorption sites and causing an increase in the dye adsorption. A negatively charged site on the adsorbent does not favour the adsorption of anionic dyes due to the electrostatic repulsion [20-22]. Hence, all the succeeding investigations were performed at pH 2.

### III.3 Effect of dosage

Fig. 4B explains the effect of dosage on the removal percentage of RhB and AO7. It was apparent from the graph that the removal of both dyes increased with an increase in dosage. This can be attributed to increase in the number of sorption sites available for the adsorption of both dyes. Also, when the dosage was increased from 0.020 to 0.140 g/L, the removal of RhB increased from 55.05 % to 93.68 % and for AO7 increased from 50.82 % to 91.8 %, respectively. Similar trends were observed for the removal of RhB and AO7 using different adsorbents [23-24].

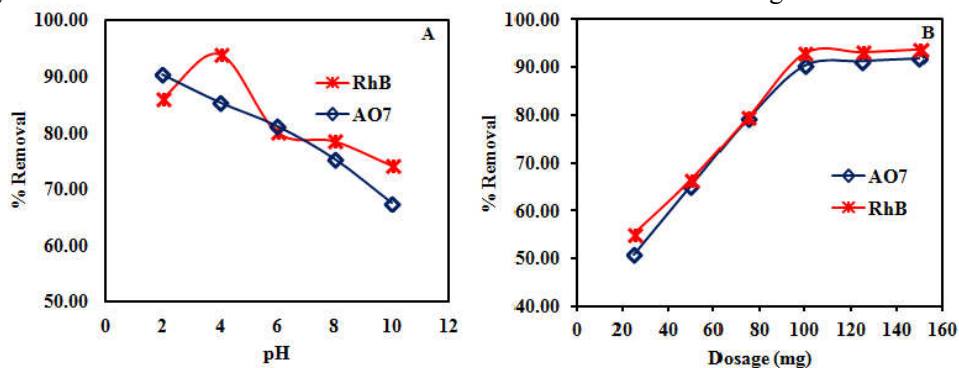


Fig.4- (A) Effect of pH (B) Effect of Dosage

### III.4. Effect of contact time and concentration

Fig. 4C and D shows the effect of contact time with 0.1 g of BAC and different initial concentrations on the removal of RhB and AO7. It is evident from the graphs that the removal of RhB and AO7 were rapid increased with increase in contact time. The adsorption process with BAC was almost finished within 60 min and small amount of RhB and AO7 uptake were observed at longer time. It also indicates that the time required to reach equilibrium depends on initial dye concentration. These results revealed that the percentage removal of two dyes mainly depends on the number of active adsorption sites available on the sorbent surface for the sorption. Hence, based on these results, the optimum contact time for the removal of two dyes using BAC was fixed as 60 min for the further adsorption studies and the initial dye concentration was fixed as 10 mg/L.

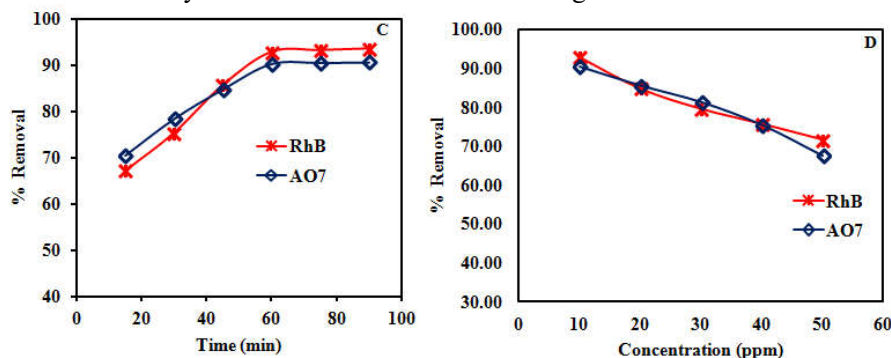


Fig 4 - (C) Effect of Contact time (D) Effect of Concentration

### III.5. Effect of Co-anions

The effect of the presence of common anions like chloride, carbonate, and bicarbonate on the removal of two dyes RhB and AO7 were studied by adding a fixed 200 mg/L initial concentration of each selected ion and a 50 mg/L initial dye concentration at room temperature and keeping all other parameters constant. Fig. 4E shows that the dye removal percentage was slightly altered by the presence of co-anions competition with the surface binding sites and hence a slight reduction in dye removal was observed.

### III.6. Adsorption isotherm

Adsorption isotherm plays major role in the design of adsorption system and also it provides the maximum sorption capacity for BAC for the removal of RhB and AO7 from aqueous solution. Many isotherm models have been used to describe the adsorption process. However, among the numerous isotherm models Langmuir and Freundlich models have been widely employed to describe the adsorption equilibrium process.

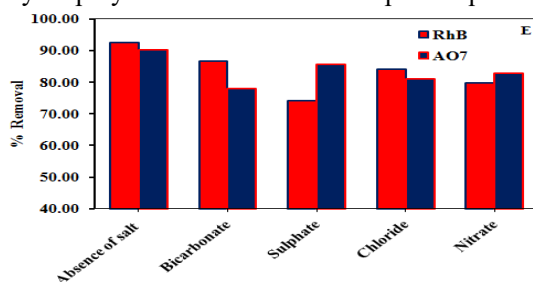


Fig.4- (E) Effect of co-anions on the RhB and AO7 removal using BAC

#### III.6.1. Langmuir isotherm

The most popular linear form of the Langmuir isotherm [25] is represented by Eq. (3):

$$\frac{C_e}{q_e} = \frac{1}{Q^0 b} + \frac{C_e}{Q^0} \quad (3)$$

Where,  $C_e$  is the equilibrium concentration of dye solution (mg/L),  $q_e$  is the amount of dye adsorbed per unit weight of the sorbent (mg/g),  $Q^0$  is the amount of adsorbate at complete monolayer coverage (mg/g) and gives the maximum sorption capacity of sorbent and  $b$  (L/mg) is Langmuir isotherm constant that relates to the energy of adsorption.

To identify the feasibility of the adsorption process, the essential characteristics of the Langmuir isotherm can be expressed in terms of the dimensionless separation factor or equilibrium parameter,  $R_L$ .

$$R_L = \frac{1}{1 + bC_0} \quad (4)$$

Where,  $b$  (L mg<sup>-1</sup>) is Langmuir isotherm constant and  $C_0$  (mg L<sup>-1</sup>) is initial concentration of dye.

The calculated values for Langmuir isotherm parameters are given in Table 1. The  $R_L$  values of Langmuir lies between 0 and 1 indicating that the adsorption process is favourable. The value of  $Q^0$  is decreased with the increase in temperature indicate the exothermic nature of the adsorption process. The obtained value of Langmuir isotherm constant (b) for RhB adsorption was higher than for AO7 adsorption in all three temperatures, which illustrate that the BAC had more affinity towards AO7 rather than RhB since the b is directly proportional to the binding energy.

### III.6.2. Freundlich isotherm

The linear form Freundlich isotherm [26] is represented by Eq. (5):

$$\log q_e = \log k_F + \frac{1}{n} \log C_e \quad (5)$$

Where,  $k_F$  is the measure of adsorption capacity and  $1/n$  is the adsorption intensity. The obtained values for Freundlich isotherm parameters are given in Table 1. The magnitude of the exponent  $1/n$  lies between 0 and 1 indicates the favourable conditions for the adsorption. The exothermic nature of the adsorption process is further confirmed by the  $k_F$  value which is decreased with an increase in temperature.

### III.7. Chi-square ( $\chi^2$ ) analysis

$\chi^2$  analysis [27] was carried out to identify the suitable isotherm model for describing the removal of RhB and AO7 from aqueous solution using BAC. The  $\chi^2$  values provide the significant information about the suitability of the isotherm model.

The mathematical expression for the  $\chi^2$  analysis is represented by Eq. (6)

$$\chi^2 = \sum \frac{(q_e - q_{e,m})^2}{q_{e,m}} \quad (6)$$

Table 1- Freundlich and Langmuir constants of BAC

Isotherm	Parameters	RhB			AO7		
		303 K	313 K	323 K	303 K	313 K	323 K
Freundlich	1/n	0.560	0.726	0.789	0.655	0.747	0.842
	$k_F$ (mg/g) (L/mg) <sup>1/n</sup>	4.922	2.76	1.99	3.96	2.50	1.69
	$r^2$	0.999	0.999	0.999	0.995	0.998	0.998
	$\chi^2$	0.033	0.036	0.046	0.094	0.086	0.068
Langmuir	$Q^0$ (mg/g)	11.99	11.51	11.36	26.95	32.21	46.47
	$b$ (L/g)	0.355	0.236	0.184	0.161	0.075	0.034
	$r^2$	0.992	0.997	0.992	0.999	0.997	0.993
	$R_L$	0.26	0.347	0.404	0.437	0.626	0.786
	$\chi^2$	8.33	8.46	8.62	22.96	21.23	20.12

Where,  $K^0$  is the sorption distribution coefficient,  $\Delta G^0$  is the standard free energy change of sorption ( $\text{kJ mol}^{-1}$ ),  $T$  is the temperature in K,  $R$  is the universal gas constant ( $8.314 \text{ J mol}^{-1} \text{ K}^{-1}$ ),  $\Delta H^0$  is the standard enthalpy change ( $\text{kJ mol}^{-1}$ ) and  $\Delta S^0$  is standard entropy change ( $\text{kJ mol}^{-1} \text{ K}^{-1}$ ). The values of  $\Delta H^0$  and  $\Delta S^0$  can be obtained from the slope and intercept of a plot of  $\ln K^0$  against  $1/T$ . The obtained values for  $\Delta G^0$ ,  $\Delta H^0$  and  $\Delta S^0$  are listed in Table 2.

The negative values of  $\Delta G^0$  indicate the removal of RhB and AO7 by BAC is a spontaneous process. The negative and positive value of  $\Delta H^0$  confirmed the exothermic and endothermic nature of the RhB and AO7 sorption process, respectively. It has also been stated that the value of  $\Delta H^0$  provides useful information about the type of adsorption process. The typical range of  $\Delta H^0$  value for physisorption is between 2.1 and 20.9 kJ/mol and for chemisorption involving complexation is between 20.9 and 418.4 kJ/mol [28-30]. The  $\Delta H^0$  values were obtained by this study, which falls within the range of physical adsorption. i.e. electrostatic interaction between BAC and both dyes. In addition, the negative and positive values of  $\Delta S^0$  indicates a decrease and increase in randomness at solid/solution interface and no significant changes occurs in the internal structure [30] during the RhB and AO7 sorption onto BAC.

### III.8. Sorption dynamics

#### III.8.1. Reaction-based models

The most commonly used pseudo-first-order and pseudo-second-order models were employed to explain the solid/liquid adsorption based.

pseudo-first-order equation of Lagergren [31] is generally expressed as:

$$\log(q_e - q_t) = \log q_e - k_{ad} \frac{t}{2.303} \quad (9)$$

Where,  $q_e$  and  $q_t$  are the adsorption capacity ( $\text{mg g}^{-1}$ ) of the sorbent at equilibrium and at time  $t$  (min), respectively,  $k_{ad}$  is the equilibrium rate constant of the pseudo-first-order sorption ( $\text{min}^{-1}$ ).

Pseudo-second-order model was also generally applied to fit the experimental data. The linear form of pseudo-second-order model [32] can be expressed as:

$$\frac{t}{q_t} = \frac{1}{h} + \frac{t}{q_e} \quad (10)$$

Where,  $q_t = (q_e^2 kt)/(1 + q_e kt)$ , the amount of dye adsorbed on the surface of the BAC at any time,  $t$  ( $\text{mg g}^{-1}$ ),  $k$  is the pseudo-second-order rate constant ( $\text{g mg}^{-1} \text{min}^{-1}$ ) and the initial sorption rate,  $h = k q_e^2$  ( $\text{mg g}^{-1} \text{min}^{-1}$ ).

**Table 2 – Thermodynamic parameters of BAC**

Thermodynamic parameters	RhB	AO7
$\Delta G^\circ$ ( $\text{kJ mol}^{-1}$ )	303 K	-5.23
	313 K	-7.49
	323 K	-8.95
$\Delta H^\circ$ ( $\text{kJ mol}^{-1}$ )	-18.71	19.95
$\Delta S^\circ$ ( $\text{kJ mol}^{-1} \text{K}^{-1}$ )	-0.19	0.18

The values obtained for the pseudo-first-order and pseudo-second-order kinetic models are given in Table 3. It can be seen from the table that the correlation co-efficient ( $r$ ) value obtained by pseudo-second-order model is higher than the pseudo-first-order model in all the studied conditions. In addition, the  $q_{e, \text{cal}}$  values obtained by pseudo-second-order model are closer to that of the  $q_{e, \text{exp}}$  values indicated that the pseudo-second-order model was better at describing the sorption system.

### III.8.2. Diffusion-based models

In a solid–liquid sorption process the transfer of solute is characterized by pore diffusion or particle diffusion control.

The pore diffusion model used here was proposed by Weber and Morris [33]. The linear form of the equation is represented by:

$$q_t = k_i t^{0.5} \quad (11)$$

Where,  $k_i$  is the intraparticle rate constant ( $\text{mg g}^{-1} \text{min}^{-0.5}$ ). The slope of the plot of  $q_t$  against  $t^{0.5}$  will give the value of intraparticle rate constant.

A particle diffusion controlled sorption process [25] is represented by the equation:

$$\ln(1 - \frac{C_t}{C_e}) = -k_p t \quad (12)$$

Where,  $C_t$  and  $C_e$  are the dye concentration at time  $t$  and equilibrium, respectively, and  $k_p$  is the particle rate constant ( $\text{min}^{-1}$ ). The value of particle rate constant is obtained by the slope of the plot of  $\ln(1 - C_t/C_e)$  against  $t$ .

The straight line plots of  $\ln(1 - C_t/C_e)$  vs.  $t$  and  $q_t$  vs.  $t^{0.5}$  indicate the applicability of both particle and intraparticle diffusion models. The  $k_p$ ,  $k_i$  and  $r$  values of particle and intraparticle diffusion models are



**Table 3- Kinetic parameters of BAC at different temperatures with different initial concentrations**

Dye	Kinetic models	Parameters	303 K				313 K				323 K			
			10 mg/L	20 mg/L	30 mg/L	40 mg/L	10 mg/L	20 mg/L	30 mg/L	40 mg/L	10 mg/L	20 mg/L	30 mg/L	40 mg/L
RhB	Pseudo-first-order	$k_{ad} (\text{min}^{-1})$	0.015	0.014	0.017	0.021	0.013	0.035	0.013	0.011	0.016	0.029	0.014	0.021
		r	0.997	0.996	0.998	0.993	0.996	0.953	0.989	0.999	0.996	0.981	0.996	0.999
	Pseudo-second-order	$q_e (\text{mg/g})$	3.803	8.021	8.545	10.228	3.806	6.554	8.061	9.179	3.711	5.903	7.621	9.008
		$k \times 10^{-2} (\text{g/mg min})$	0.028	0.021	0.023	0.021	0.021	0.016	0.018	0.020	0.019	0.021	0.016	0.016
		$h (\text{mg/g min})$	0.400	1.375	1.679	2.198	0.305	0.708	1.158	1.686	0.268	0.742	0.924	1.288
		r	0.998	0.999	0.999	0.999	0.996	0.998	0.998	0.999	0.997	0.999	0.998	0.999
AO7	Pseudo-first-order	$k_{ad} (\text{min}^{-1})$	0.010	0.027	0.036	0.028	0.012	0.016	0.026	0.024	0.011	0.061	0.027	0.046
		r	0.997	0.983	0.945	0.945	0.995	0.990	0.978	0.994	0.993	0.873	0.970	0.910
	Pseudo-second-order	$q_e (\text{mg/g})$	3.800	6.946	8.981	10.363	3.704	6.005	8.627	9.967	3.407	5.992	8.139	9.183
		$k \times 10^{-2} (\text{g/mg min})$	0.024	0.016	0.021	0.023	0.020	0.025	0.026	0.032	0.027	0.024	0.030	0.031
		$h (\text{mg/g min})$	0.341	0.754	1.683	2.460	0.275	0.904	1.956	3.177	0.313	0.873	2.009	2.574
		r	0.996	0.998	0.999	0.999	0.995	0.998	0.999	0.999	0.996	0.999	0.999	0.999

**Table 4- Particle and Intraparticle kinetic model parameters of BAC at different temperatures with different initial concentrations**

Dye	Kinetic models	Parameters	303 K				313 K				323 K			
			10 mg/L	20 mg/L	30 mg/L	40 mg/L	10 mg/L	20 mg/L	30 mg/L	40 mg/L	10 mg/L	20 mg/L	30 mg/L	40 mg/L
RhB	Particle diffusion	$k_p (\text{min}^{-1})$	0.517	0.698	1.337	1.543	0.566	1.069	1.385	1.592	0.518	1.020	1.404	1.599
		r	0.997	0.997	0.992	0.993	0.992	0.999	0.999	0.994	0.995	0.997	0.999	0.980
		sd	0.036	0.030	0.013	0.009	0.067	0.007	0.005	0.007	0.053	0.011	0.005	0.015
	Intraparticle diffusion	$k_i (\text{mg/g min}^{0.5})$	1.900	5.287	5.870	7.269	1.596	3.432	4.996	6.181	1.370	3.328	4.261	5.293
		r	0.998	0.995	0.999	1.000	0.998	0.997	0.994	1.000	0.999	0.999	0.999	0.995
		sd	0.026	0.056	0.028	0.019	0.032	0.048	0.070	0.011	0.017	0.019	0.034	0.083
AO7	Particle diffusion	$k_p (\text{min}^{-1})$	0.610	1.110	1.292	1.505	0.601	1.023	1.217	1.443	0.389	0.956	1.189	1.470
		r	0.991	0.995	0.999	0.999	0.992	1.000	0.998	0.992	0.993	0.998	0.999	0.999
		sd	0.061	0.023	0.005	0.002	0.059	0.004	0.006	0.007	0.044	0.010	0.003	0.002
	Intraparticle diffusion	$k_i (\text{mg/g min}^{0.5})$	1.764	3.630	6.167	7.772	1.468	3.801	6.285	7.912	1.604	3.660	6.112	7.148
		r	0.996	0.995	0.997	0.992	0.994	0.995	0.999	0.998	0.994	0.999	0.998	0.997
		sd	0.037	0.071	0.042	0.070	0.049	0.047	0.018	0.026	0.040	0.023	0.027	0.036

illustrated in Table 4. The higher  $r$  values obtained for both particle and intraparticle diffusion models suggest that BAC composite follow both the models on dye sorption.

#### IV. Conclusions

The possibility of prepared BAC as an adsorbent for the removal of RhB and AO7 from aqueous solution was investigated by batch method. The pH of the reaction was found to play a major role in the RhB and AO7 dyes removal process and the optimum pH for the removal of RhB was at pH 4 and for AO7 it was at pH 2. The results obtained for RhB and AO7 dyes sorption successfully fit the Freundlich isotherm model than the Langmuir model. The thermodynamic parameters ( $\Delta G^\circ$ ,  $\Delta H^\circ$ , and  $\Delta S^\circ$ ) of RhB adsorption indicated that the system was exothermic in nature and at the same time the adsorption process of AO7 was endothermic. Subsequently the kinetic data fit to pseudo-second-order model and the sorption process was controlled by the pattern of both particle and intra-particle diffusion. Based on these results, the prepared BAC can be considered as potential adsorbent to remove RhB and AO7 dyes effectively from industrial effluent.

#### References

1. Wang, S., Zhu, Z.H., *Effects of acidic treatment of activated carbons on dye adsorption. Dyes Pigments.* 75, 306–314 (2007).
2. Janos P, Buchtova H and Ryznarova M, *Water Res.*, 37(20), 4938-4944, (2003)
3. Santhy K and Selvapathy P, *Bioresour Technol.*, 97, 1329-133 (2006)
4. Grag, V.K., Renuka Gupta., Anu Bala yadav., Rakesh Kumar. "Dye removal from aqueous solution by adsorption on treated sawdust." *Bioresource Technology*, 89 (2), 121124 (2003)
5. Y.Guo, S. Yang, W. Fu, J. Qi, R. Li, Z. Wang and H.xu. *Dyes Pigments*, 56, 219 (2003).
6. G. Mckay. *J. Chem. Technol. Biotechnol.*, 32, 759 (1982).
7. F. K. Bangash and A. Manaf. *Jour. Chem, Soc. Pak.*, 26, 111 (2004).
8. F. K Bangash and S. Alam, *Tenside Surf, Det.*, 43, 299 (2006).
9. F. K Bangash and S. Alam, I.Ahmad, *Chin. J. Chem.*, 25, 596, (2007).
10. V.Meshko, L. Markovska, M.Mincheva and A. E. Rodrigues, *Wat. Res.*, 35, 3357 (2001).
11. Deniz, F., Saygideger, S.D. *Equilibrium, kinetic and thermodynamic studies of Acid Orange 52 dye biosorption by Paulownia tomentosa Steud leaf powder as a low-cost natural biosorbent. Bioresour. Technol.* 101, 5137–5143 (2010).
12. Hameed, B.H., Ahmad, A.A., Aziz, N. *Adsorption of reactive dye on palm-oil industry waste: equilibrium, kinetic and thermodynamic studies. Desalination* 247, 551–560 (2009).
13. Han, R., Zhang, L., Song, C., Zhang, M., Zhu, H., Zhang, L. *Characterization of modified wheat straw, kinetic and equilibrium study about copper ion and methylene blue adsorption in batch mode. Carbohydr. Polym.* 79, 1140–1149 (2010).
14. Tahir, H., Sultan, M., Jahanzeb, Q. *Removal of basic dye methylene blue by using bioabsorbents Ulva lactuca and Sargassum. Afr. J. Biotechnol.* 7, 2649–2655 (2008).
15. Gad, H. M. H.; El-Sayed, A. A. *Activated carbon from agricultural by-products for the removal of Rhodamine-B from aqueous solution. J. Hazard. Mater.* 168, 1070–1081 (2009)
16. Kumar, R.; Mago, G.; Balan, V.; Wyman, C.E.;. *Physical and chemical characterizations of corn stover and poplar solids resulting from leading pretreatment technologies. Bioresource Technology.* 100 (17), 3948–3962 (2009).
17. Gad, H. M. H.; El-Sayed, A. A. *Activated carbon from agricultural by-products for the removal of Rhodamine-B from aqueous solution. J. Hazard. Mater.* 168, 1070–1081 (2009).
18. Eftekhari, S.; Habibi-Yangjeh, A.; Sohrabnezhad, S. *Application of AlMCM-41 for competitive adsorption of methylene blue and rhodamine B: Thermodynamic and kinetic studies. J. Hazard. Mater.* 178, 349–355 (2010).
19. Guo, Y.; Zhao, J.; Zhang, H.; Yang, S.; Qi, J.; Wang, Z.; Xu, H. *Use of rice husk-based porous carbon for adsorption of Rhodamine B from aqueous solutions. Dyes Pigment.* 66, 123–128 (2005).
20. Arami, M.; Limaee, N.Y.; Mahmoodi, N.M.; Tabrizi, N.S. *Removal of dyes from colored textile wastewater by orange peel adsorbent: equilibrium and kinetics studies. J. Colloid Interface Sci.* 288, 371–376 (2005).

21. Namasivayam, C.; Kavitha, D. Removal of Congo Red from water by adsorption onto activated carbon prepared from coir pith, an agricultural solid waste. *Dyes Pigments* 54, 47–58 (2002).
22. Yenikaya, C.; Atar, E.; Olgun, A.; Atar, N.; Ilhan, S.; Çolak, F. Biosorption study of anionic dyes from aqueous solutions using *Bacillus amyloliquefaciens*, *Eng. Life Sci.* 10 233–241 (2010).
23. El Haddad, M., Mamouni, R., Saffaj, N. and Lazar, S., *Global J. Human Soc. Sci. Geography Environ. Geo Sci.*, 12(10), 18-29 (2012).
24. Yahya Hamzeh, Alireza Ashori, Elham Azadeh, Ali Abdulkhani. Removal of Acid Orange 7 and Remazol Black 5 reactive dyes from aqueous solutions using a novel biosorbent. *Materials Science and Engineering C* 32 1394–1400 (2012).
25. I. Langmuir, The constitution and fundamental properties of solids and liquids, *J. Am. Chem. Soc.* 38, 2221–2295 (1916).
26. H.M.F. Freundlich, Über die adsorption in l'ösungen, *Z. Phys. Chem.* 57A 385–470 (1906).
27. Rathinam Karthik, Sankaran Meenakshi, Removal of Pb(II) and Cd(II) ions from aqueous solution using polyaniline grafted chitosan, *Chemical Engineering Journal* 263, 168–177 (2015).
28. Kumar, R.; Ansari, M.O.; Barakat, M.A. DBSA doped polyaniline/multi-walled carbon nanotubes composite for high efficiency removal of Cr(VI) from aqueous solution, *Chem. Eng. J.* 228, 748–755 (2013).
29. Sun, C.; Li, C.; Wang, C.; Qu, R.; Niu, Y.; Hongbo, G. Comparison studies of adsorption properties for Hg(II) and Au(III) on polystyrene-supported bis-8-oxyquinoline-terminated open-chain crown ether, *Chem Eng. J.*, 200–202 (200) 291 (2012)
30. Alkan, M., Demirbas, O., Dogan, M. Adsorption kinetics and thermodynamics of an anionic dye onto sepiolite. *Microporous and Mesoporous Materials*, 101 (3), 388–396 (2007).
31. Lagergren, S. Zur theorie der sogenannten adsorption gelöster stoffe, *K. Sven. Vetenskapsakad. Handl.* 24 1–39 (1898).
32. Ho. Y.S. Second - order kinetic model for the sorption of cadmium onto tree fern: a comparison of linear and non-linear methods, *Water Res.*, 40, 119–125 (2006).
33. Weber, W.J.; Morris, J.C. Kinetics of adsorption of carbon from solution, *J. Saint. Eng. Div. ASCE* 89, 31–59 (1963).